Peptidoglycan synthesis in *Mycobacterium tuberculosis* is organized into networks with varying drug susceptibility

Karen J. Kieser[a], Catherine Baranowski[a], Michael C. Chao[b], Jarukit E. Long[c], Christopher M. Sassetti[c,d], Matthew K. Waldor[b,d,e], James C. Sacchettini[f], Thomas R. Ioerger[g], and Eric J. Rubin[a,e,1]

[a]Department of Immunology and Infectious Disease, Harvard T. H. Chan School of Public Health, Boston, MA 02115; [b]Division of Infectious Diseases, Brigham & Women's Hospital, Boston, MA 02115; [c]Department of Microbiology and Physiological Systems, University of Massachusetts Medical School, Worcester MA 01655; [d]Howard Hughes Medical Institute, Chevy Chase, MD 20815; [e]Department of Microbiology and Immunobiology, Harvard Medical School, Boston, MA 02115; [f]Department of Biochemistry and Biophysics and Department of Chemistry, Texas A&M University, College Station, TX 77843; and [g]Department of Computer Science, Texas A&M University, College Station, TX 77843

Peptidoglycan (PG), a complex polymer composed of saccharide chains cross-linked by short peptides, is a critical component of the bacterial cell wall. PG synthesis has been extensively studied in model organisms but remains poorly understood in mycobacteria, a genus that includes the important human pathogen *Mycobacterium tuberculosis* (*Mtb*). The principle PG synthetic enzymes have similar and, at times, overlapping functions. To determine how these are functionally organized, we carried out whole-genome transposon mutagenesis screens in *Mtb* strains deleted for *ponA1*, *ponA2*, and *ldtB*, major PG synthetic enzymes. We identified distinct factors required to sustain bacterial growth in the absence of each of these enzymes. We find that even the homologs PonA1 and PonA2 have unique sets of genetic interactions, suggesting there are distinct PG synthesis pathways in *Mtb*. Either PonA1 or PonA2 is required for growth of *Mtb*, but both genetically interact with LdtB, which has its own distinct genetic network. We further provide evidence that each interaction network is differentially susceptible to antibiotics. Thus, *Mtb* uses alternative pathways to produce PG, each with its own biochemical characteristics and vulnerabilities.

Mycobacterium tuberculosis | transposon sequencing | genetic interaction | peptidoglycan | cell wall

One of the leading causes of infectious disease deaths worldwide is tuberculosis (TB), caused by *Mycobacterium tuberculosis* (*Mtb*). One-third of the human population is thought to harbor *Mtb* and ~1.5 million individuals died of TB last year (1). *Mtb*'s success as a pathogen is due in part to its unusual cell wall, which is notorious for its complexity and is implicated in *Mtb*'s innate resistance to many commonly used antibiotics (2). A critical component of the bacterial cell wall (including *Mtb*'s) is peptidoglycan (PG), a complex polymer that provides structural support and counteracts turgor pressure (3). PG is essential for cell survival, and its synthesis is targeted by many potent antibiotics (2).

PG consists of long glycan chains composed of two different sugars (Fig. 1*A*) that are cross-linked via short peptide side chains that extend from the glycan chains. Notably, generation of mature PG occurs outside of the cell membrane and is mediated by enzymes that incorporate new PG subunits, which are formed in the cytoplasm, into the PG polymer. PonA1 and PonA2 are the two enzymes in *Mtb* that can both polymerize glycan strands and cross-link peptides [known as bifunctional penicillin binding proteins (PBPs), Fig. 1*A*]. The predominant peptide cross-links in mycobacteria join the third amino acids (3–3 link) of adjacent stem peptides (4, 5), which are synthesized by L,D-transpeptidases (Ldts) such as LdtB, one of the major Ldts in *Mtb* (Fig. 1*A*). The peptides can also be joined by cross-linking the fourth and third amino acids (4–3 link) (Fig. 1*A*) through the action of bifunctional or monofunctional (capable of only peptide cross-linking) PBPs. The activity of these distinct factors must be coordinated to ensure proper cell-wall synthesis. One method of coordination is the use of large protein complexes, the elongation complex and divisome, which mediate cell-wall biogenesis during cell elongation or division, respectively (2). The essential activity of these enzymes makes them prime drug targets; indeed, PBPs and Ldts are inhibited by carbapenems and penicillin (6, 7), which remains one of the most clinically important drugs in use.

Although the biosynthesis and structure of PG have been investigated for decades, predominantly in organisms such as *Escherichia coli* or *Bacillus subtilis*, the mechanisms that coordinate the biochemical activities required to polymerize and modify the cell wall remain incompletely understood. Moreover, much less is known about PG synthesis in many pathogenic organisms, including *Mtb* (2). However, previous studies in *Mtb* suggest that PG synthesis in this pathogen does not strictly conform to the *E. coli* paradigm. For example, *E. coli* has three bifunctional PBPs [PBP1A, PBP1B, and PBP1C (3)], whereas *Mtb* has just two [PonA1 and PonA2 (8)]. Additionally, PBP2 (known as PBPA in mycobacteria) is a monofunctional PBP and is required for cell elongation in *E. coli*, but instead seems to function in cell septation in mycobacteria (3, 9).

The structure of PG is also different in *Mtb* than in *E. coli*: Mycobacterial PG has an unusual prevalence of 3–3 peptide linkages. The abundance of 3–3 cross-links in mycobacterial PG throughout different growth stages (5) suggests that Ldts are

Significance

The rise of drug-resistant *Mycobacterium tuberculosis* (*Mtb*) underscores the critical need for a better understanding of essential physiological processes. Among these is cell-wall synthesis, the target of many antibiotics. To understand how *Mtb* orchestrates synthesis of its cell wall, we performed whole-genome interaction studies in cells with different peptidoglycan synthesis mutations. We found that different enzymes become required for bacterial growth in Δ*ponA1*, Δ*ponA2*, and Δ*ldtB* cells, suggesting that discrete cell envelope biogenesis networks exist in *Mtb*. Furthermore, we show that these networks' enzymes are differentially susceptible to cell-wall–active drugs. Our data provide insight into the essential processes of cell-wall synthesis in *Mtb* and highlight the role of different synthesis networks in antibiotic tolerance.
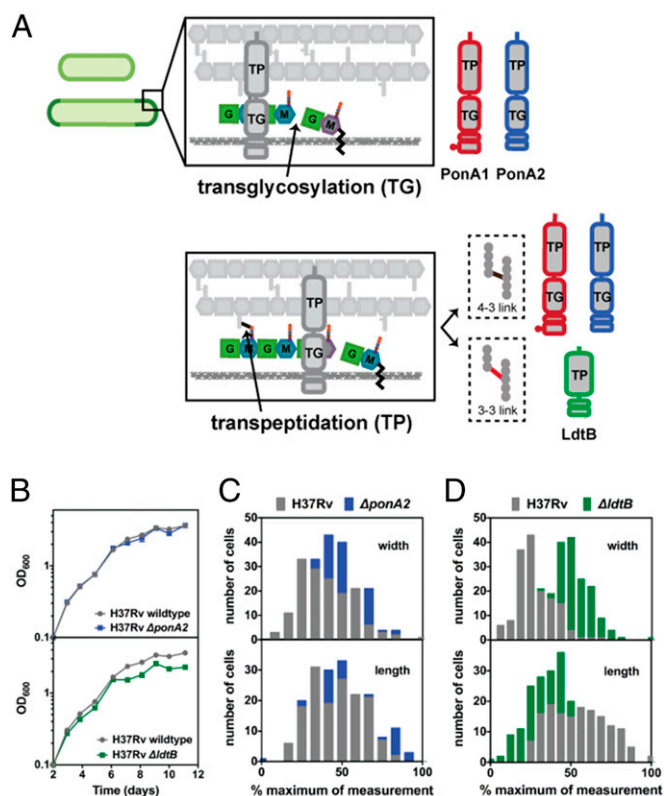
MICROBIOLOGY

Fig. 1. Deletion of PG synthases influences growth and morphology of *Mtb*. (*A*) Transglycosylation (TG) and transpeptidation (TP) reactions incorporate new PG subunits into the cell wall. PonA1 and PonA2 carry out both TG and 4–3 TP reactions. LdtB only mediates 3–3 TP reactions. M, N-acetylmuramic acid. G, N-acetylglucosamine. (*B*) Deletion of either *ponA2* or *ldtB* does not greatly affect *Mtb* growth during log phase, although loss of *ldtB* reduces population density in stationary phase. Error bars are often too small to see. (*C*) *ponA2* mutant cells (*n* = 179) have increased width compared with wild-type cells (*n* = 153) (approximate *P* value <0.0001 by the Kolmogorov–Smirnov test). (*D*) *ldtB* mutant cells (*n* = 193) have increased width and decreased length compared with wild-type cells (*n* = 153) (approximate *P* value <0.0001 by the Kolmogorov–Smirnov test for both length and width).

active during normal growth; however, their cellular roles or regulation during growth and PG biogenesis remain largely unknown. Whereas penicillins and cephalosporins target only enzymes that produce 4–3 cross-links, Ldts can be targeted by carbapenems (7). Recent work suggests that these agents might be far more efficacious against both dividing and nondividing bacteria (10). Although little is known about *Mtb*'s five encoded Ldts (11), one, LdtB, is implicated in antibiotic tolerance (11–13), is required for normal virulence in a mouse model of TB (12), and is important for normal cell shape (13).

Previous studies have also revealed that PG biosynthesis differs between *Mtb* and the related saprophytic *Mycobacterium smegmatis* (*Msm*). As opposed to *Mtb*, *Msm* has three bifunctional PBPs: PonA1, PonA2, and PonA3 (14). PonA1 is required for *Msm* but not *Mtb* growth in culture (15, 16); however, PonA1 is required for robust growth of *Mtb* during infection (16). In contrast, *Mtb* and *Msm ponA2* mutants do not have growth defects in culture (14, 17). However, *Mtb* strains with inactivated *ponA1* or *ponA2* exhibit similar survival defects during growth in a host (16, 18), suggesting that these two similar bifunctional enzymes have nonredundant and important contributions to PG synthesis during infection. Collectively, the differences in PG synthase functionality may imply that different PG synthetic pathways exist across species, which may have consequences for a pathogen's virulence during infection.

Here, we interrogated PG synthesis in *Mtb* by investigating the genetic interactions of *ponA1*, *ponA2*, and *ldtB*, which encode three PG synthases critical for *Mtb*'s growth during infection. To identify these interactions, we performed genome-wide transposon mutagenesis screens in *Mtb* mutant strains that lacked one of these enzymes. Advances in high-throughput sequencing technology coupled with the power of whole-genome studies provide unique insights into key bacterial processes, such as cell-wall biosynthesis. Such studies have been performed to a limited extent in bacteria, and further work would substantially expand our understanding of the organization of prokaryotic metabolic processes. In this study, we identified diverse genetic interaction networks for *ponA1*, *ponA2*, and *ldtB*, suggesting that these synthases are embedded within distinct cellular networks for assembling *Mtb*'s PG. We found that either *ponA1* or *ponA2* is required for cell growth, and that *ldtB* interacts with both *ponA1* and *ponA2*. Moreover, mutants that lack these enzymes have differential susceptibility to agents that interfere with cell-wall biogenesis. Thus, the *Mtb* cell wall is synthesized using multiple interacting networks that are both overlapping and unique.

Results

PonA1, PonA2, and LdtB Are Individually Dispensable for Growth of *Mtb*. PonA1, its homolog PonA2, and LdtB can generate bonds between new PG subunits and those in the existing PG polymer (Fig. 1*A*). We generated independent *ponA2* and *ldtB* deletion mutants and assessed their growth. As suggested by previous studies (14, 18) absence of either gene did not substantially affect *Mtb*'s exponential growth, although loss of LdtB diminished population density in stationary phase (Fig. 1*B*). However, Δ*ponA2* cells were moderately wider than wild-type *Mtb* (Fig. 1*C*). In contrast, Δ*ponA1* cells are longer than wild-type cells (16), suggesting these two homologous enzymes have distinct roles in PG synthesis in *Mtb*. Mutant cells that lack LdtB were significantly shorter [as previously reported (13)] and wider than wild-type cells (Fig. 1*D*), indicating that LdtB affects cell-wall synthesis in a manner distinct from the two bifunctional PBPs. Thus, even though deletion of *ponA1* (16), *ponA2*, or *ldtB* is compatible with cell growth, their individual deletions have detectable and distinct physiological effects.

Whole-Genome Mutagenesis Identifies PG Biogenesis Pathways in *Mtb*. In *E. coli*, the PonA1 and PonA2 homologs, PBP1a and PBP1b, seem to function in different subcellular complexes and have been shown to have distinct interaction partners (3). We hypothesized that, in a similar fashion, PonA1 and PonA2 genetically interact with different pathways. To elucidate the shared and distinct roles of PonA1, PonA2, and LdtB in *Mtb* PG biogenesis, we used transposon mutagenesis and high-throughput sequencing in Δ*ponA1*, Δ*ponA2*, and Δ*ldtB Mtb* strains to define the genetic interactions of these enzymes on a genome-wide scale (19, 20) (Figs. S1 and S2). These experiments measure bacterial fitness across a population. Genes that contain fewer than expected transposon insertions have a growth disadvantage (here termed "essential") whereas those with larger numbers of insertions have an advantage ("enriched"). Comparisons of the transposon insertion profiles (21, 22) of the wild-type and mutant strains revealed both essential and enriched genes—two types of genetic interaction—in each strain (Fig. 2).

We identified 10 factors required in cells that lack PonA1 (Fig. 2*A*, essential factors). Most of these factors are associated with or predicted to be involved in cell-wall synthesis. For example, factors involved in peptidoglycan (PonA2), mycolic acid (MmaA4), and, potentially, arabinogalactan (CpsY) synthesis in addition to cell-wall precursor production (Rv1086) were found to be required in Δ*ponA1* cells (Fig. 2*A*). These data suggest that the cell requires either PonA1 or PonA2 for PG synthesis, analogous to the situation in *E. coli* (3). We also identified eight factors whose disruption in the Δ*ponA1* mutant seemed beneficial to the cell (Fig. 2*A*, enriched). For example, the transcription factor EspR (*rv3849*) had higher levels of transposon insertions in cells that lack *ponA1*
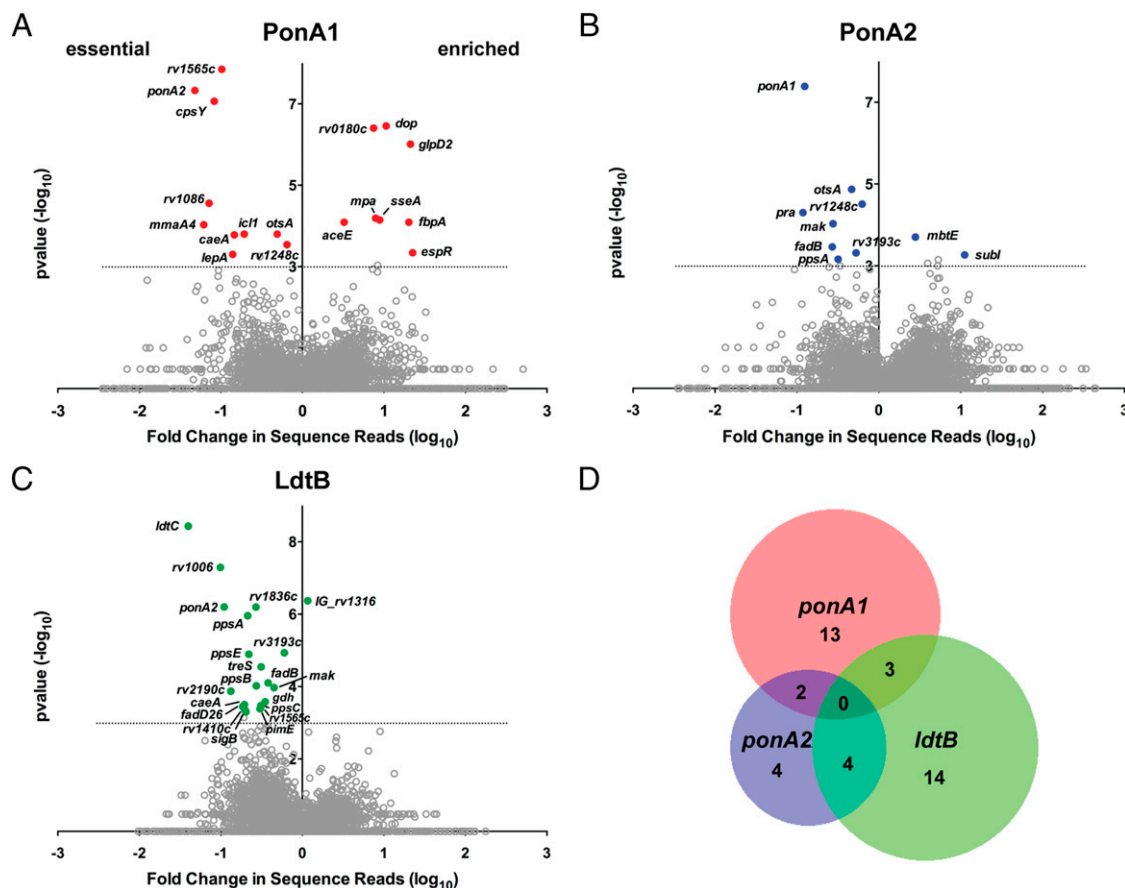
Fig. 2. *ponA1*, *ponA2*, and *ldtB* have largely distinct genetic interactions. Loci whose sequence reads were significantly different between wild-type and mutant cells [(A) Δ*ponA1*, red circles; (B) Δ*ponA2*, blue circles; (C) Δ*ldtB*, green circles] with a P value <0.001 (represented by the dotted line) by the Mann–Whitney *u* test are plotted according to their P value and fold change in sequence reads from wild type (calculated from the geometric mean). Gray circles, nonsignificant loci. Gray circles above the dotted line are loci that are <90% significant in the simulations (*SI Materials and Methods*). (D) Venn diagram representation of the distinct interaction networks of *ponA1*, *ponA2*, and *ldtB*.

compared with wild-type *Mtb*, suggesting that cells that lack EspR may grow more rapidly than wild-type cells under these conditions. This could indicate that EspR regulates *ponA1* transcription. Indeed, we found multiple canonical EspR binding sites (23) in the *ponA1* promoter region (Fig. S3).

Our screen identified widely different genetic connections for *ponA2* compared with *ponA1*. As predicted from the screen performed in Δ*ponA1* cells, *ponA1* was required in Δ*ponA2* cells (Fig. 2B). Relatively few factors were shared between Δ*ponA1* and Δ*ponA2* cells. For example, *rv3490* and *rv1248c* were required in both backgrounds. However, there were many differences, such as *cpsY*, *rv1086*, *pra*, and *fadB*, and the differences were in both the essential and enriched classes (Fig. 2 *A* and *B*). Thus, although either PonA1 or PonA2 is required for *Mtb* growth, both enzymes have predominantly different genetic interactions.

ldtB also interacts with a number of loci including some, such as *ponA2*, that overlap with *ponA1* interactions (Fig. 2C). In the absence of either of the bifunctional enzymes that form 4–3 cross-links, 3–3 cross-linking may become more important for maintaining cell integrity. In addition, *ldtB* interacts with genes involved in cell-wall precursor synthesis (*treS*) and other steps in peptidoglycan metabolism, including the NlpP60 hydrolase Rv2190c (24). Collectively, these data show that the PG synthases PonA1, PonA2, and LdtB participate in largely distinct genetic networks (Fig. 2D).

PG Synthases Are Variably Required in *ponA1*, *ponA2*, or *ldtB* Mutant Cells. We took advantage of the depth and saturation of the mutant libraries to establish the relative contributions of PBPs

and Ldts to bacterial fitness in the different mutant strain backgrounds. We analyzed the frequency of transposon insertions in the four PBP and five Ldt loci as well as a putative penicillin binding protein (Rv2864c) in each mutant strain. We found that particular PG synthases had differential insertion profiles in cells that lack *ponA1*, *ponA2*, or *ldtB* (Fig. 3). For example, transposon disruption of *pbpA* generated a relative growth disadvantage in *ponA1* mutant cells compared with wild type whereas transposon disrupted *pbpA* exhibited growth advantages in *ponA2* and *ldtB* mutant cells. These data suggest that PBPA may be more important for PG synthesis in cells without PonA1 than in cells without PonA2 or LdtB. Our data also support a role for *rv2864c* in PG synthesis. In *ponA1* mutant cells, *rv2864c* was disrupted at just 15% of the wild-type frequency but was disrupted at 82% or 51% of the wild-type frequency in *ponA2* or *ldtB* mutant cells, respectively (Fig. 3).

PonA2 Is Required for PG Synthesis in the Absence of PonA1. We chose select genes for individual validation of essentiality using a previously described allelic exchange method (16, 25) (Fig. 4A and Fig. S4). For example, we generated a *ponA2* deletion in a strain whose only copy of *ponA1* is at the L5 phage integration site (Δ*ponA1* L5::*ponA1_{wt}*). We also generated a *ponA2* deletion in wild-type H37Rv *Mtb* as a control. We assessed the impact of *ponA2* loss in the mutant background and found that Δ*ponA1* L5::*ponA1_{wt}* Δ*ponA2* cells grew at rates similar to and exhibited rod-shaped morphology similar to wild-type *Mtb* (Fig. S5 *A* and *B*). However, although we could integrate a wild-type *ponA1* copy into the L5 site in Δ*ponA2* or Δ*ponA1* L5::*ponA1_{wt}* Δ*ponA2* backgrounds
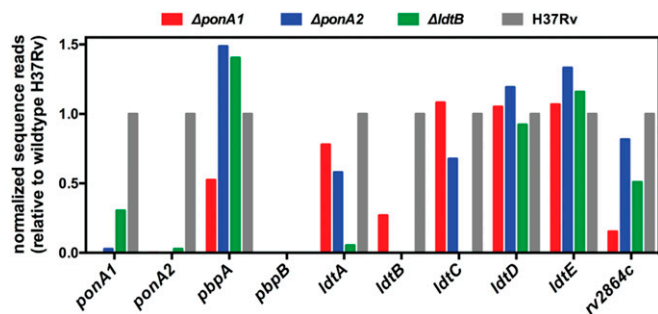
Fig. 3. Importance of PG synthases in *ponA1*, *ponA2*, or *ldtB* mutant cells. Sequence reads corresponding to transposon insertions at the indicated loci in the Δ*ponA1*, Δ*ponA2*, and Δ*ldtB* mutant cells. Sequence reads at each locus are normalized to the respective locus in wild-type H37Rv cells.

(Fig. 4B and Fig. S6A), when we transformed an L5 empty vector we only obtained a significant number of colonies in the Δ*ponA2* cells that still encode *ponA1* at the original locus (Fig. 4B and Fig. S6A). This confirms that PonA2 is required in the absence of PonA1 in *Mtb* and that even though these enzymes participate in largely distinct genetic networks they have at least partially complementary roles in PG biogenesis in *Mtb*.

Rv1086 Is Required for Cell-Wall Synthesis in Cells That Lack PonA1.
Rv1086, a *Z*-isoprenyl diphosphate synthase, carries out the first committed step in the synthesis of the lipid carrier for cell-wall precursors (26). As with *ponA2*, we used allelic exchange to test whether *rv1086* was required in cells that lack *ponA1* (Fig. 4C). Indeed, we obtained robust growth only when we transformed Δ*ponA1* L5::*ponA1*$_{wt}$ Δ*rv1086* cells [which grew similarly to and exhibited cell shape similar to wild-type *Mtb* (Fig. S5 C–E)] with another *ponA1* copy (Fig. 4D and Fig. S6B). These data demonstrate that *rv1086* is required in cells that lack *ponA1* and may indicate that PonA2 requires a dedicated pool of precursors.

LdtB Is Critical for Normal Bacterial Fitness in Cells Without PonA1.
An important prediction of the findings from our Δ*ponA1* and Δ*ponA2* screens is that both strains require *ldtB* for optimal growth (Fig. 4E and Fig. S7). Whereas bifunctional PBPs are critical in many bacterial species (3), mycobacterial PG exhibits very different architecture with its prevalence of 3–3 cross-links (4, 5). Using allelic exchange, we found that only tiny Δ*ponA1* Δ*ldtB* colonies could be seen after 21 d of growth, when Δ*ldtB* colonies were already large (Fig. 4F and Fig. S6C); these colonies required 35 d to reach a similar size (Fig. S6D). Thus, *ldtB* is required for robust growth in the absence of *ponA1*.

Distinct Cell-Wall Synthesis Networks Exhibit Differential Tolerance to Cell-Wall–Active Drugs. Our data suggest that PonA1, PonA2, and LdtB participate in distinct genetic networks with partially overlapping but largely unique genetic interactions for each enzyme. We hypothesized that these networks would have different cellular activity and could therefore be differentially susceptible to drugs that target cell-wall synthesis. To test this hypothesis, we treated cells that lack *ponA1*, *ponA2*, *ldtB*, or other members of their interaction networks with drugs that inhibit the various components of *Mtb*'s cell wall, including meropenem, which blocks PG transpeptidases; teicoplanin, which binds directly to PG to prevent further cross-linking (10, 27); ethambutol, which targets arabinogalactan synthesis; and isoniazid, which targets mycolic acid synthesis. We found that Δ*ponA1* cells had the same minimum inhibitory concentration (MIC) for meropenem and teicoplanin as wild-type *Mtb* (Fig. 5); however, Δ*ponA2* and Δ*ldtB* cells were four- to eightfold more susceptible to both meropenem and teicoplanin. Furthermore, mutants that lack *ponA1* exhibit a fourfold increased susceptibility to ethambutol. However, the Δ*ponA2* or Δ*ldtB* mutants do not exhibit heightened sensitivity

to this antibiotic. Δ*ponA1*, Δ*ponA2*, or Δ*ldtB* cells exhibited no change in MIC when treated with SDS, and only Δ*ldtB* cells were slightly more sensitive to isoniazid. The Δ*rv1086* mutant was eightfold more sensitive to teicoplanin and fourfold more sensitive to meropenem and ethambutol compared with wild-type *Mtb* (Fig. 5). Together, these data suggest that the enzymes that comprise distinct PG synthetic networks have different roles in antibiotic tolerance in *Mtb*.

Discussion

Cell-wall synthesis requires the collaboration of multiple enzymes. In most bacterial species, individual PBPs are dispensable. This is generally interpreted as evidence of functional redundancy, suggesting that enzymes have overlapping functions. Clearly, this is not entirely true in both *Msm* and *Mtb*. In *Msm*, a single bifunctional PBP, PonA1, is essential for normal growth, but *ponA1* and *ponA2* are both required for robust growth of *Mtb* during infection. Our network analysis suggests that PonA1 and PonA2 are not identical—each is genetically associated with overlapping and, importantly, unique factors. This may suggest that although PonA1 and PonA2 mediate similar reactions, the pathways by which each synthesizes PG are different. This likely has functional consequences for bacterial growth in specific conditions. Indeed, we found that mutant cells exhibit differential survival under
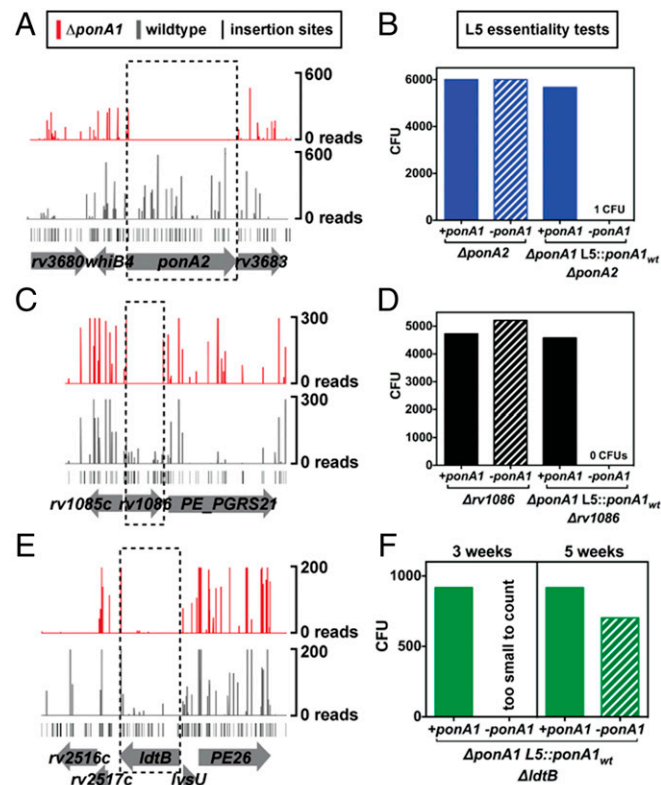
Fig. 4. Diverse cell-wall synthesis factors become required in Δ*ponA1* cells. (*A*) Transposon insertions (vertical bars), determined from high-throughput sequencing, are visualized at the *ponA2* locus in either wild-type (gray) or Δ*ponA1* (red) cells. (*B*) Colony-forming units (CFUs) were counted from allelic exchanges with L5-integrating vectors that do or do not encode *ponA1* in the experimental Δ*ponA1* L5::*ponA1*$_{wt}$ Δ*ponA2* strain or the control Δ*ponA2* strain (both control strain transformations had lawn growth, and CFUs were arbitrarily set to 6,000). (*C*) Transposon insertions at the *rv1086* locus in wild-type (gray) and Δ*ponA1* (red) cells. (*D*) CFU counts from L5 allelic exchanges in the experimental Δ*ponA1* L5::*ponA1*$_{wt}$ Δ*rv1086* strain or the control Δ*rv1086* strain. (*E*) Transposon insertions at the *ldtB* locus in wild-type (gray) or Δ*ponA1* (red) cells. (*F*) CFU counts from L5 allelic exchanges in the experimental Δ*ponA1* L5::*ponA1*$_{wt}$ Δ*ldtB* strain.
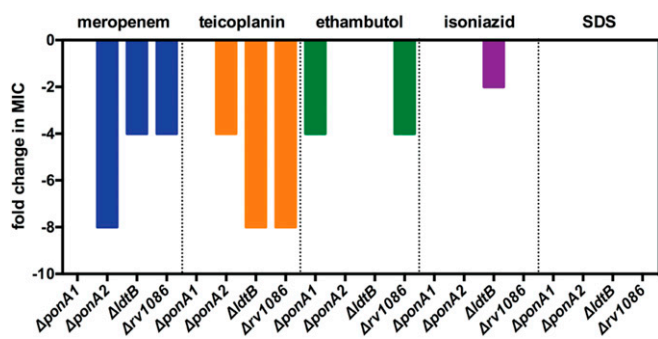
Fig. 5. Differential susceptibility of *Mtb* cell-wall mutants to cell-wall–active antibiotics. The fold change in MIC for the indicated drugs and SDS were calculated compared with wild-type *Mtb* for the indicated strains.

antibiotic treatment, suggesting that cell-wall synthesis enzymes, even closely related homologs, exhibit different functionality during *Mtb* growth. This is likely true for other bacterial species as well. Furthermore, we found that both *ponA1* and *ponA2* are genetically associated with *ldtB*. This suggests that the bifunctional PBPs function together with this major 3–3 transpeptidase to synthesize new PG during growth.

What do these genetic interactions mean? They may imply separate biochemical pathways that, for example, provide precursors to PonA1 and PonA2. Several pieces of evidence indicate that PonA1 and PonA2 have distinct cellular roles, including their susceptibilities to host-like stresses or infection (14) as well as structural differences (28) and different impacts on cell shape (Fig. 1) (16). These data may support a model wherein PonA1 and PonA2 exist in different subcellular complexes (3). Our genetic analyses also support different cellular roles for PonA1 and PonA2. Notably, few interactions were identical for *ponA1* and *ponA2*, suggesting their cellular activities are not truly redundant (Fig. 6). Because a fully redundant system would unlikely be maintained through evolution, there is likely some selective advantage to having multiple independent systems for PG synthesis (in *Mtb* and other organisms). There could be several reasons for this. For example, these proteins could be individually regulated, either transcriptionally or by substrate availability provided by proteins lying within dedicated synthesis pathways. This could result in altered rates of PG formation and, consequently, growth, or could result in a different structure of PG. For example, loss of 4–3 cross-links could increase the importance of 3–3 cross-links for cell-wall integrity. This model is consistent with the relative importance of *ldtB*, one of the major 3–3 cross-linking enzymes, with loss of either *ponA1* or *ponA2*.

ldtB is the single Ldt that becomes critical for growth in the absence of *ponA1* or *ponA2* (Fig. 3). The genetic interaction between the bifunctional PBPs and *ldtB* suggests that these enzymes together promote new cell-wall synthesis during growth. This may indicate that new glycan strands (synthesized by PonA1 or PonA2) are predominantly first cross-linked in a 3–3 manner (for example, by LdtB). This model is supported by the prevalence of 3–3 cross-links in mycobacterial PG at all growth stages (5). Our data also show that LdtB is critical for the maintenance of normal cell shape (Fig. 1), which suggests that LdtB holds a key role in cell-wall synthesis. Such 3–3 peptide cross-links, which also exist in other bacteria, may provide increased structural integrity to the cell during adverse conditions.

Whereas the cellular changes brought about by mutation are the ends of the spectrum, it is likely that the balance between PonA1 and PonA2 activity is altered under different growth conditions. This produces bacilli that can closely adapt to particular growth conditions. For example, although there is little effect on growth rate in culture, loss of PonA1 or PonA2 results in attenuation during murine infection. This could be associated with changes in cell morphology that are observed even in culture or could be specific for interactions between the cell wall and the host.

A specific example of adaptation is the presence of antibiotics. Mutant cells have altered susceptibility to some antibiotics (Figs. 5 and 6). It is possible that this is due to altered bacterial permeability. However, these differences are mainly specific for drugs that affect the synthesis of cell-wall components and not the detergent SDS, suggesting that increased susceptibility is actually caused by changes in the requirement for specific cell-wall synthetic enzymes in the presence of mutations. The differential antibiotic response of *ponA1* and *ponA2* mutant cells further supports a model wherein they exist in separate PG synthesis pathways. For example, *ponA2* mutant cells are more sensitive to meropenem and teicoplanin than *ponA1* mutant cells. This suggests that these drugs may more efficiently inhibit the active enzymes in Δ*ponA2* cells (including PonA1) than the remaining enzymes in Δ*ponA1* cells. These observations suggest that inhibition of PG synthesis by transpeptidase inhibitors such as β-lactam or glycopeptide antibiotics could synergize with other cell-wall biosynthesis inhibitors and increase their efficacy. Understanding the pathways involved could help to design such synergistic pairs of inhibitors—for *Mtb* as well as other bacterial pathogens, many of which have not been subjected to similar studies. Efforts to target these pathogens could ultimately profit from similar strategies to identify novel members of key metabolic pathways and define individual contributions to antibiotic tolerance.

Materials and Methods

Bacterial Strains and Growth Conditions. *M. tuberculosis* H37Rv and *E. coli* Top10 (Invitrogen; used for cloning) were cultured as in ref. 16. The construction of the Δ*ponA1* and Δ*ponA1* L5::*ponA1*$_{wt}$ *Mtb* strains was described in ref. 16.

Transposon Mutagenesis. The H37Rv transposon libraries were generated using the φMycoMarT7 phagemid as previously described (29).

Genomic Library Construction and High-Throughput Sequencing. Genomic DNA (gDNA) was harvested from the transposon libraries and prepared for PCR amplification as described (19). PCR-amplified transposon–gDNA junctions were then subjected to high-throughput sequencing (Illumina). For additional details of library preparation and data analysis, see *SI Materials and Methods*.

Mapping and Counting Transposon Insertions. Sequence data were filtered for transposon-specific information and trimmed of transposon sequence except for the TA dinucleotide insertion site with custom Python scripts (*SI Appendix*, sections 1, 2, and 3). Trimmed reads were mapped to the H37Rv genome using Bowtie2 (30). Insertions at each genomic TA site were counted with custom Python scripts (*SI Appendix*, sections 4 and 5).

Analysis of Differentially Inserted Genes. Loci that were differentially disrupted between wild-type and mutant cells were assessed as in ref. 22 (Dataset S1). We used the Mann–Whitney *u* test and simulation-based normalization without the hidden Markov model (HMM) (22). For each library's locus, the geometric
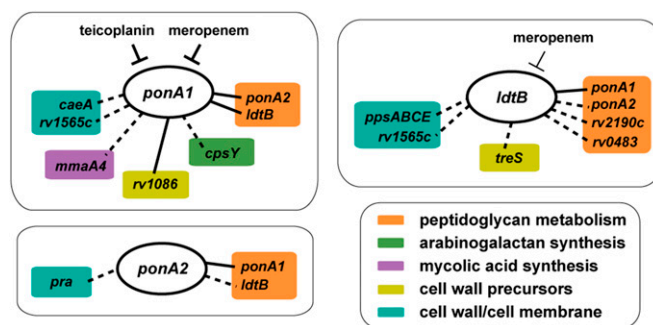
Fig. 6. *ponA1*, *ponA2*, and *ldtB* are hubs of distinct cell-wall synthesis networks. Selected interactions with cell-wall synthesis genes discovered in whole-genome screens (dashed lines) and/or by directed knockouts (solid lines) for *ponA1*, *ponA2*, and *ldtB*. The members of these networks respond differently to specific cell-wall drugs, such as teicoplanin and meropenem. For example, meropenem may target PonA1 more (thicker "T") than LdtB (thinner "T").

MICROBIOLOGY

mean of the sequence reads was calculated (Dataset S2) with a custom MATLAB script using the encoded geomean function (*SI Appendix*, section 10).

Recombinant DNA Constructs and Gene Knockouts. *ponA1* was subcloned into the L5 pMC1s vector as in ref. 16. The *ponA2* knockout cassette was amplified by PCR from a custom phage (31). The *rv1086* and *ldtB* knockout cassettes consisted of 500 nucleotides 5′ or 3′ of *rv1086* or *ldtB* flanking a hygromycin cassette with *PmeI* sites at each end (Gen9). Digestion with *PmeI* (New England Biolabs) generated linear recombineering products. The *ponA2*, *ldtB*, and *rv1086* deletions were generated in the Δ*ponA1* L5::*ponA1_{wt}* strain (16) via recombineering (for more details, see *SI Materials and Methods*).

Allelic Exchange in *Mtb*. Allelic exchange occurs as described (16, 23). The Δ*ponA1* L5::*ponA1_{wt}* loxed strain wherein *ponA2*, *rv1086*, or *ldtB* was deleted was used for allelic exchange. Simultaneous control transformations with the same L5 vectors were performed in Δ*ponA2*, Δ*rv1086*, and Δ*ldtB* cells. Colony-forming units were counted at 21 d, except for the Δ*ponA1* L5::*tetR* Δ*ldtB* plate, which was counted at 35 d.

Optical Density Measurements. Population growth curves for *Mtb* strains were performed as in ref. 16.

Light Microscopy and Image Analysis. Cells were fixed overnight in 1% formalin at 4 °C in the Biosafety Level 3 facility. Cells were imaged and morphology analyzed as in ref. 16. Final images were prepared in Fiji (32).

Antibiotic MIC Assays. The antibacterial effects of meropenem, teicoplanin, ethambutol, isoniazid, and SDS (Sigma Aldrich) were determined as in ref. 16.

Data Representation and Statistical Analysis. Prism 6.0 (GraphPad Software) was used to graph and analyze numerical data. Statistical tests in Prism calculated significance of measurements as reported in figure legends. The Venn diagram was generated with BioVenn (33). Transposon insertions were visualized in DNAplotter (34) or Artemis (35) by converting the insertion counts to appropriate data structures with custom Python scripts (*SI Appendix*, sections 8 and 9).

1. World Health Organization (2014) *Global Tuberculosis Report* (World Health Organization, Geneva).
2. Kieser KJ, Rubin EJ (2014) How sisters grow apart: Mycobacterial growth and division. *Nat Rev Microbiol* 12(8):550–562.
3. Typas A, Banzhaf M, Gross CA, Vollmer W (2012) From the regulation of peptidoglycan synthesis to bacterial growth and morphology. *Nat Rev Microbiol* 10(2):123–136.
4. Lavollay M, et al. (2008) The peptidoglycan of stationary-phase Mycobacterium tuberculosis predominantly contains cross-links generated by L,D-transpeptidation. *J Bacteriol* 190(12):4360–4366.
5. Kumar P, et al. (2012) Meropenem inhibits D,D-carboxypeptidase activity in Mycobacterium tuberculosis. *Mol Microbiol* 86(2):367–381.
6. Dubée V, et al. (2012) Inactivation of Mycobacterium tuberculosis l,d-transpeptidase LdtMt₁ by carbapenems and cephalosporins. *Antimicrob Agents Chemother* 56(8):4189–4195.
7. Wivagg CN, Bhattacharyya RP, Hung DT (2014) Mechanisms of β-lactam killing and resistance in the context of Mycobacterium tuberculosis. *J Antibiot (Tokyo)* 67(9):645–654.
8. Cole ST, et al. (1998) Deciphering the biology of Mycobacterium tuberculosis from the complete genome sequence. *Nature* 393(6685):537–544.
9. Dasgupta A, Datta P, Kundu M, Basu J (2006) The serine/threonine kinase PknB of Mycobacterium tuberculosis phosphorylates PBPA, a penicillin-binding protein required for cell division. *Microbiology* 152(Pt 2):493–504.
10. Hugonnet J-E, Tremblay LW, Boshoff HI, Barry CE, 3rd, Blanchard JS (2009) Meropenem-clavulanate is effective against extensively drug-resistant Mycobacterium tuberculosis. *Science* 323(5918):1215–1218.
11. Sanders AN, Wright LF, Pavelka MS, Jr (2014) Genetic characterization of mycobacterial L,D-transpeptidases. *Microbiology* 160(Pt 8):1795–1806.
12. Gupta R, et al. (2010) The Mycobacterium tuberculosis protein LdtMt2 is a nonclassical transpeptidase required for virulence and resistance to amoxicillin. *Nat Med* 16(4):466–469.
13. Schoonmaker MK, Bishai WR, Lamichhane G (2014) Nonclassical transpeptidases of Mycobacterium tuberculosis alter cell size, morphology, the cytosolic matrix, protein localization, virulence, and resistance to β-lactams. *J Bacteriol* 196(7):1394–1402.
14. Patru MM, Pavelka MS, Jr (2010) A role for the class A penicillin-binding protein PonA2 in the survival of Mycobacterium smegmatis under conditions of nonreplication. *J Bacteriol* 192(12):3043–3054.
15. Hett EC, Chao MC, Rubin EJ (2010) Interaction and modulation of two antagonistic cell wall enzymes of mycobacteria. *PLoS Pathog* 6(7):e1001020.
16. Kieser KJ, et al. (2015) Phosphorylation of the peptidoglycan synthase PonA1 governs the rate of polar elongation in mycobacteria. *PLoS Pathog* 11(6):e1005010.
17. Vandal OH, Pierini LM, Schnappinger D, Nathan CF, Ehrt S (2008) A membrane protein preserves intrabacterial pH in intraphagosomal Mycobacterium tuberculosis. *Nat Med* 14(8):849–854.
18. Vandal OH, et al. (2009) Acid-susceptible mutants of Mycobacterium tuberculosis share hypersusceptibility to cell wall and oxidative stress and to the host environment. *J Bacteriol* 191(2):625–631.
19. Long JE, et al. (2015) Identifying essential genes in Mycobacterium tuberculosis by global phenotypic profiling. *Methods Mol Biol* 1279:79–95.
20. Joshi SM, et al. (2006) Characterization of mycobacterial virulence genes through genetic interaction mapping. *Proc Natl Acad Sci USA* 103(31):11760–11765.
21. Chao MC, et al. (2013) High-resolution definition of the Vibrio cholerae essential gene set with hidden Markov model-based analyses of transposon-insertion sequencing data. *Nucleic Acids Res* 41(19):9033–9048.
22. Pritchard JR, et al. (2014) ARTIST: High-resolution genome-wide assessment of fitness using transposon-insertion sequencing. *PLoS Genet* 10(11):e1004782.
23. Blasco B, et al. (2012) Virulence regulator EspR of Mycobacterium tuberculosis is a nucleoid-associated protein. *PLoS Pathog* 8(3):e1002621.
24. Parthasarathy G, et al. (2012) Rv2190c, an NlpC/P60 family protein, is required for full virulence of Mycobacterium tuberculosis. *PLoS One* 7(8):e43429.
25. Pashley CA, Parish T (2003) Efficient switching of mycobacteriophage L5-based integrating plasmids in Mycobacterium tuberculosis. *FEMS Microbiol Lett* 229(2):211–215.
26. Schulbach MC, et al. (2001) Purification, enzymatic characterization, and inhibition of the Z-farnesyl diphosphate synthase from Mycobacterium tuberculosis. *J Biol Chem* 276(15):11624–11630.
27. Dong SD, et al. (2002) The structural basis for induction of VanB resistance. *J Am Chem Soc* 124(31):9064–9065.
28. Calvanese L, et al. (2014) Structural and binding properties of the PASTA domain of PonA2, a key penicillin binding protein from Mycobacterium tuberculosis. *Biopolymers* 101(7):712–719.
29. Sassetti CM, Boyd DH, Rubin EJ (2001) Comprehensive identification of conditionally essential genes in mycobacteria. *Proc Natl Acad Sci USA* 98(22):12712–12717.
30. Langmead B, Salzberg SL (2012) Fast gapped-read alignment with Bowtie 2. *Nat Methods* 9(4):357–359.
31. Jain P, et al. (2014) Specialized transduction designed for precise high-throughput unmarked deletions in Mycobacterium tuberculosis. *MBio* 5(3):e01245–e14.
32. Schindelin J, et al. (2012) Fiji: An open-source platform for biological-image analysis. *Nat Methods* 9(7):676–682.
33. Hulsen T, de Vlieg J, Alkema W (2008) BioVenn - a web application for the comparison and visualization of biological lists using area-proportional Venn diagrams. *BMC Genomics* 9:488.
34. Carver T, Thomson N, Bleasby A, Berriman M, Parkhill J (2009) DNAPlotter: Circular and linear interactive genome visualization. *Bioinformatics* 25(1):119–120.
35. Carver T, Harris SR, Berriman M, Parkhill J, McQuillan JA (2012) Artemis: An integrated platform for visualization and analysis of high-throughput sequence-based experimental data. *Bioinformatics* 28(4):464–469.